2014 IEEE International Conference on Robotics & Automation (ICRA)
Hong Kong Convention and Exhibition Center
May 31 - June 7, 2014. Hong Kong, China

Longitudinal Wheel-slip Control for Four Wheel Independent Steering and Drive Vehicles

Tin Lun Lam, *Member, IEEE,* Huihuan Qian, *Member, IEEE,* and Yangsheng Xu, *Fellow, IEEE*

***Abstract*— In this paper, a longitudinal wheel-slip controller for four wheel independent steering and drive (4WISD) vehicles is proposed to suppress longitudinal wheel slip in varying road conditions. Different from conventional methods that consider single driving source and zero steering angle, the proposed controller considers all independent traction sources from each driving wheel and omnidirectional steering command so as to eliminate slip detection errors in 4WISD vehicles. The proposed controller requires low cost sensing equipment, including merely wheel speed sensor and accelerometer, which makes the system practical to be utilized. The proposed wheel-slip controller can be applied to vehicles with arbitrary quantity of driving wheels and different steering configurations such as traditional two-front-wheel steering and two-rear-wheel steering. Numerical simulation results are presented to demonstrate the efficiency of the proposed longitudinal wheel-slip controller.**

I. Introduction

Longitudinal wheel-slip in automobile reduces the driving efficiency. Most importantly, it reduces the controllability due to the reduction of the side force and hence results in a vehicle accident. Longitudinal wheel-slip occurs when the driving torque exceeds a limit. It has a high tendency to happen when the friction of coefficient between road and tires is low such as on the wet or icy roads. As a result, a proper control of the traction force to eliminate wheel slip in real time is important to enhance vehicle safety.

In recent decades, due to the awareness of the environmental protection, electric-motor driven vehicles become popular. When compared with traditional internal combustion engines, a quicker response and more precise of torque generation can be achieved by electric motors. Many researchers take these control merits to design anti-slip controllers on electric vehicles. Zheng [1] and Amodeo [2] proposes traction controllers to avoid serious wheel slip. In that, the wheel slip is detected by comparing the difference between the wheel spinning speed and actual vehicle speed. However, in vehicle control, the most headache issue is how to obtain the actual vehicle speed. In current technology, obtaining the actual vehicle speed directly is not practical. Bevly [3] adopts Global Positioning System (GPS) to provide speed information. However, the information is not accurate enough and the sampling rate is low. Optical-based sensors, such as the one proposed by Joos [4] can provide the velocity information with high sampling rate and more precise, but it needs frequent cleaning maintenance and the measurement accuracy is affected by the texture of the road surface and weather such as raining.

In view of the limitations of the current technologies in measuring the actual vehicle speed directly, researchers tend to detect the wheel slip according to easily obtained information, such as wheel torque and speed as proposed in [5], [6], [7], [8], [9]. These methods require the mathematical models of the vehicle body, wheel, and the road surface condition. Most of the works are working on a simplified one-wheel-car model only and a zero steering angle is assumed. There is not much discussion of the longitudinal wheel slip issue on four wheel independent steering and drive (4WISD) vehicles which have omnidirectional steerability and independent controllability of the traction force on each wheel. It will result in an inaccurate detection of the wheel slip if these methods are applied on each wheel of 4WISD vehicles independently as this approach neglects the force required for vehicle turning and the coupling effect of the traction force from other wheels.

As 4WISD configuration permits high maneuverability, it is one of the popular configurations in wheeled mobile robots such as [10]. The independent control of the traction force is beneficial for optimizing the driving efficiency [11] and improving vehicle stability [12], [13], [14], [15]. In recent decade, numbers of 4WISD vehicles were developed such as Toyota Fine-T, Nissan Pivo2 and OK-1 [16]. It is believed that the 4WISD configuration will become a popular setting in future electric vehicles.

In view of the lack of anti-slip technology for 4WISD vehicles, we propose a novel longitudinal wheel-slip controller for 4WISD vehicles which considers all independent traction sources from driving wheels and omnidirectional steering command. It can generally be applied to vehicles that are driven by arbitrary quantity of standard wheels [17] and with different steering configurations such as traditional front-wheel steering and rear-wheel steering. The proposed wheel-slip controller includes the longitudinal wheel-slip detector, re-adhesion detector, and the re-adhesion control algorithm. Different from the conventional anti-slip controllers that only constrain the traction force below the peak value as shown in Fig. 1, the proposed re-adhesion control can recover the wheel slip even if a serious slip occurs, (slip ratio is far out

T. Lam is with the Smart China Research, Smart China (Holdings) Limited, Hong Kong, China. tinlun.lam@smartchinaholdings.com

H. Qian and Y. Xu are with the Department of Mechanical and Automation Engineering, The Chinese University of Hong Kong; and Shenzhen Institutes of Advanced Technology, Chinese Academy of Sciences. hhqian@mae.cuhk.edu.hk, ysxu@mae.cuhk.edu.hk

This paper is partially supported by GHP/009/11GD, Hong Kong Innovation and Technology Fund, and RFD 2013/2014, Centre for research on Robotics and Smart-city, The Chinese University of Hong Kong - Smart China.

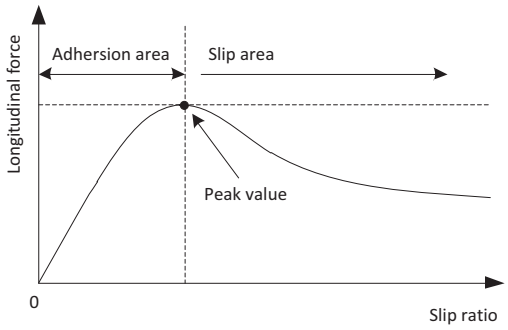

Fig. 1. Relationship between slip ratio and traction force.

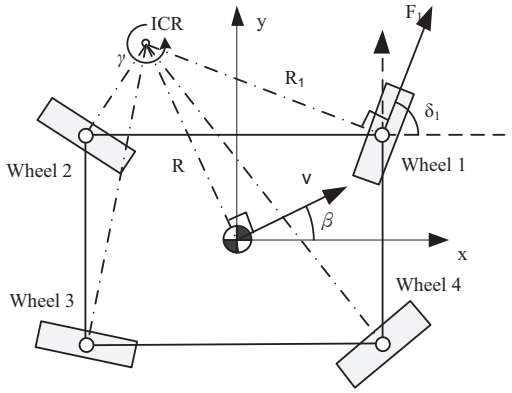

Fig. 2. Configuration of 4WISD vehicles.

of the adhesion area). On top of that, the proposed controller requires low cost sensing equipment only, that is wheel speed sensor and accelerometer, which make the system practical to be utilized.

The remainder of this paper is organized as follows. Section II describes the dynamic model of a 4WISD vehicle. The proposed longitudinal wheel-slip detector for 4WISD vehicles is presented in Section III. The proposed re-adhesion detector is addressed in Section IV and the re-adhesion control algorithm is presented in Section V. In Section VI, numerical simulation results are presented to evaluate the performance of the proposed wheel-slip controller. Finally, conclusion is given in Section VII.

II. Modeling of 4WISD Vehicle

A 4WISD vehicle is driven by four standard wheels. The traction force of each wheel is controlled by an in-wheel motor independently. The orientations of wheels can also be adjusted about their vertical axes independently. This configuration permits the vehicle to turn about an arbitrary instantaneous center of rotation (ICR). This capability is named omnidirectional steering. Fig. 2 shows a schematic diagram of a 4WISD vehicle. The origin of the coordinate system is located at the center of mass of the vehicle. R is the turning radius, i.e., the horizontal distance between the center of mass and the ICR. R_i is the horizontal distance between the ICR and the center of wheel i. v and γ represents the tangential velocity and yaw rate respectively. β denotes the heading angle of the vehicle body. δ_i is the orientation of wheel i. F_i denotes the longitudinal traction force on a wheel. The location of the target ICR $({}^tx_{ICR}, {}^ty_{ICR})$ is defined by steering inputs $\phi = \begin{bmatrix} \phi_1 & \phi_2 & \phi_3 \end{bmatrix}$,

$$\begin{bmatrix} {}^tx_{ICR} \\ {}^ty_{ICR} \end{bmatrix} = \begin{bmatrix} \phi 3 - \cot\phi 1 \cdot \sin\phi 2 \\ \cot\phi 1 \cdot \cos\phi 2 \end{bmatrix} \tag{1}$$

The relationship among the target ICR and the steering inputs in detail can be found in [18].

A. Vehicle Body Dynamics

A planar motion is considered in the vehicle modeling, hence the roll, pitch and vertical motions are neglected. In addition, as we are focusing on evaluating the longitudinal slip of wheel, it is assumed that the lateral slip is minor in all wheels such that the motion of vehicle body will almost follow the steering command. The equation of motion of a vehicle body is described as

$$RF_{air} + \sum_{i=1}^{n} R_i F_i = \left(I + mR^2\right) \frac{d\gamma}{dt} \tag{2}$$

In that, n is the quantity of driving wheel (n=4 in 4WISD vehicles), I is the moment of inertia of the vehicle body about the center of mass, m is the mass of the vehicle, R_i is the distance between the center of wheel i and the target ICR, F_{air} is the drag force resulted by air resistance which is defined as

$$F_{air} = -C_{air} v^2 \tag{3}$$

where C_{air} is a coefficient of air resistance.

B. Wheel Modeling

The longitudinal traction force F_i is related to the slip ratio of a wheel. It can be approximated by the magic formula proposed by Pacejka [19],

$$F_i = f(\sigma_i) = D\sin(C\arctan\{B\sigma_i - E[B\alpha - \arctan(B\sigma_i)]\}) \tag{4}$$

where B, C, D, and E represent the coefficient of stiffness, shape, peak and curvature respectively. In that, D is proportional to the coefficient of friction μ between the tire and road surface. σ_i is the slip ratio on wheel i which is defined as

$$\sigma_i = \frac{r\omega_i - v}{v} \tag{5}$$

where r is the radius of a wheel which is assumed to be identical and constant in all wheels in this paper. ω_i is the spinning speed of wheel i.

The relationship among longitudinal traction force, wheel output torque and the spinning acceleration of wheel i is defined as

$$F_i = \frac{1}{r}\left(\tau_i - J\frac{d\omega_i}{dt}\right) \tag{6}$$

where τ_i is the torque generated by the in-wheel motor in wheel i which can be obtained by measuring the motor current. J is the moment of inertia of the wheel. Table I lists the parameters of the modeling and the values adopted in the simulation.

TABLE I

THE PARAMETERS OF THE VEHICLE MODEL.

Parameter	Symbol	Unit	Value
Vehicle mass	m	kg	1200
Moment of inertia of a vehicle	I	kgm^2	1000
Coordinate of wheel 1	(x_1, y_1)	m	(1.25,0.75)
Coordinate of wheel 2	(x_2, y_2)	m	(-1.25,0.75)
Coordinate of wheel 3	(x_3, y_3)	m	(-1.25,-0.75)
Coordinate of wheel 4	(x_4, y_4)	m	(1.25,-0.75)
Coefficient of air resistance	C_{air}	-	0.45
Moment of inertia of a wheel	J	kgm^2	2.7
Radius of a wheel	r	m	0.25
Coefficient of stiffness	B	-	10
Coefficient of shape	C	-	1.9
Coefficient of peak	D	-	3000
Coefficient of curvature	E	-	-0.8

III. LONGIUDINAL WHEEL-SLIP DETECTOR

Longitudinal wheel slip in a 4WISD vehicle can be detected by using the dynamics of the wheels and the vehicle body which is introduced in Section II.
Substitute (6) into (2),

$$RF_{air} + \sum_{i=1}^{n} \left[\left(\tau_i - J\frac{d\omega_i}{dt} \right) \frac{R_i}{r} \right] = \left(I + mR^2 \right) \frac{d\gamma}{dt} \quad (7)$$

When slipping occurs on wheel j,

$$\frac{r}{R_j}\frac{d\omega_j}{dt} > \frac{d\gamma}{dt} \quad (8)$$

Substitute (8) into (7),

$$\left(I + mR^2 \right) \frac{r}{R_j}\frac{d\omega_j}{dt} > \sum_{i=1}^{n} \left[\left(\tau_i - J\frac{d\omega_i}{dt} \right) \frac{R_i}{r} \right] + RF_{air} \quad (9)$$

$$\frac{d\omega_j}{dt} > \frac{\sum_{\substack{i=1 \\ i\neq j}}^{4} \left[R_i \left(\tau_i - J\frac{d\omega_i}{dt} \right) \right] + \tau_j R_j + rRF_{air}}{\left(I + mR^2 \right) \frac{r^2}{R_j} + JR_j} \quad (10)$$

In (10), F_{air} is difficult to be measured. However, in the case of moving forward which is considered in this paper, F_{air} is assumed to be negative. As a result, the inequality (10) still holds even if F_{air} is omitted, i.e.,

$$\frac{d\omega_j}{dt} > \frac{\sum_{\substack{i=1 \\ i\neq j}}^{4} \left[R_i \left(\tau_i - J\frac{d\omega_i}{dt} \right) \right] + \tau_j R_j}{\left(I + mR^2 \right) \frac{r^2}{R_j} + JR_j} \quad (11)$$

The proposed longitudinal wheel-slip detector is then defined as (11). It requires the information of the torque and acceleration of all wheels only which are easy to be measured.

When the steering angle tends to zero, R_i, R_j and R tend to infinity. Then, (11) becomes

$$\frac{d\omega_j}{dt} > \frac{\sum_{\substack{i=1 \\ i\neq j}}^{4} \left(\tau_i - J\frac{d\omega_i}{dt} \right) + \tau_j}{J + mr^2} \quad (12)$$

When only one wheel is considered, (12) becomes

$$\frac{d\omega}{dt} > \frac{\tau}{J + mr^2} \quad (13)$$

which is identical to the conventional wheel-slip detector [20] that a single traction force and zero steering angle is assumed. It shows the generality of the proposed wheel-slip detector.

IV. INERTIAL-BASED RE-ADHESION DETECTOR

When slip occurs, the spinning speed of a wheel is no longer suitable to approximate the actual linear speed of the wheel by

$$\hat{v}_i = r\omega_i \quad (14)$$

As a result, the proposed re-adhesion detector keeps track of the vehicle acceleration and spinning speed of wheels by a 2-axis accelerometer and wheel speed sensors respectively. Once a slip is detected by the longitudinal wheel-slip detector, the time at this moment is defined as $t = 0$, and the actual linear speed of wheel i is approximated by

$$\hat{v}_i[t] = r\omega_i[0-s] + t_s \sum_{k=0-s+1}^{t} a_i[k] \quad (15)$$

where t_s is the sampling time. s is the approximation of the time that the slip does not occur yet. The time s should not be taken too long as it will increase the accumulative error. It also cannot be too short that the wheel slip may already occur at that moment. a_i is the tangential acceleration of wheel i. It can be obtained by the 2-axis accelerometer installed at the center of mass of the vehicle body. Let the two orthogonal measurements of the acceleration are lied on the x- and y-axis respectively, i.e.,

$$\vec{a}_m = \begin{bmatrix} a_x & a_y \end{bmatrix} \quad (16)$$

The tangential acceleration of wheel i is obtained by

$$a_i = \frac{R_i}{R}\left(a_x \cos\beta + a_y \sin\beta \right) \quad (17)$$

By using (15), $\hat{v}_i$ is obtained based on the wheel speed when the serious slip does not occur and the integration of the tangential acceleration of the wheel. Although the numerical integration method is well known to have an accumulative error that will gradually increase with time, most of the literature and commercial products are reported that the error is below 0.05m/s after 10s numerical integration. The duration of integration required in our application is even shorter as the longitudinal wheel slip can always be suppressed in one second by using the re-adhesion controller proposed in next section. As a result, the approximation of the actual linear speed of wheel can keep in a high accuracy.

The re-adhesion is identified when the linear speed approximated by (14) is equal to or smaller than that approximated by (15), that is

$$\omega_i[t]\, r \leq r\omega_i[0-s] + \sum_{k=0-s}^{t} a_i[k] \quad (18)$$

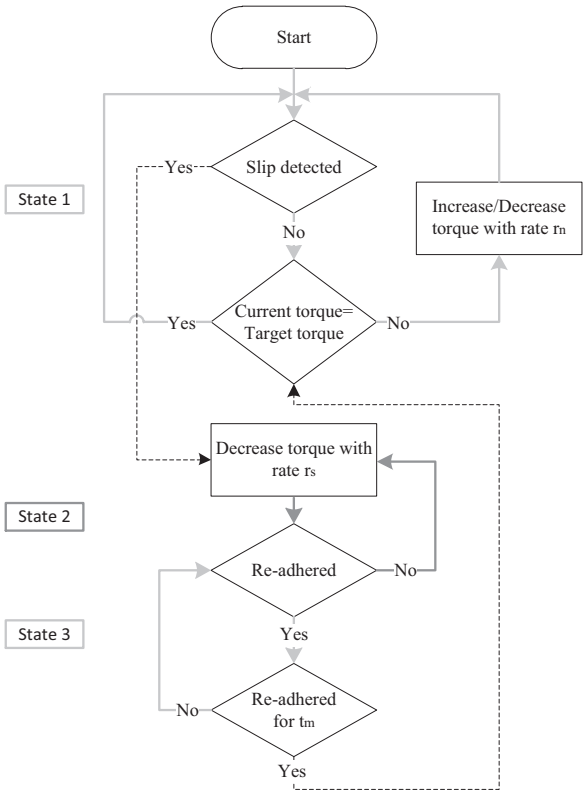

Fig. 3. Flow of the proposed wheel-slip controller.

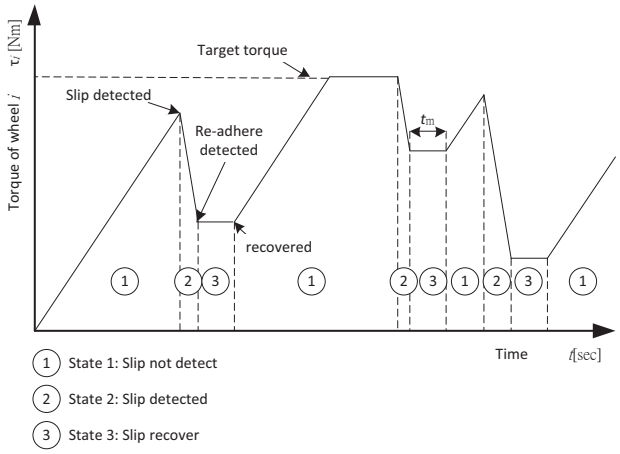

Fig. 4. An example of a torque response controlled by the proposed wheel-slip controller.

TABLE II

THE PARAMETERS OF THE LONGITUDINAL WHEEL-SLIP CONTROLLER.

Parameter	Symbol	Unit	Value
Sampling time	t_s	ms	10
Change rate of target torque in normal situation	r_n	Nm/s	1000
Change rate of target torque when slip occur	r_s	Nm/s	5000
Re-adhesion duration	t_m	ms	500
Time constant	s	ms	200

V. LONGITUDINAL WHEEL-SLIP CONTROLLER

The proposed wheel-slip controller makes use of the proposed wheel-slip detector and re-adhesion detector to control the output torque of each wheel so as to suppress longitudinal wheel slip. Fig. 3 illustrates the flow of the longitudinal wheel-slip control and Fig. 4 demonstrates a torque response in different states.

State 1: When there is no slip detected by the longitudinal wheel-slip detector, the longitudinal wheel-slip controller allows the output torque tracking the target torque by increasing or decreasing the torque gradually with a constant rate r_n.

State 2: Once a slip is identified by the longitudinal wheel-slip detector, the output torque decreases rapidly with a constant rate r_s. The longitudinal wheel-slip detector is disabled until the re-adhesion of the wheel is confirmed by the controller.

State 3: The decrease of torque pauses when the re-adhesion is identified by re-adhesion detector. The longitudinal wheel-slip controller confirms the wheel is re-adhered when re-adhesion is detected continuously for time t_m. Then, the longitudinal wheel-slip controller allows the output torque to track the target torque again and keeps check if the wheel is slipped by the longitudinal wheel-slip detector, that is, returns to State 1.

In the controller, the rate r_s should be high to shorten the time of re-adhesion. r_n should not be set too high to keep the change of torque gently. In addition, the parameters t_m should be set at least several times of the sampling time t_s. The time constant s should be smaller than t_m to avoid taking the inappropriate reference to approximate the actual linear speed of a wheel. The parameters of the longitudinal wheel-slip controller and the values used in the simulation are listed in Table II.

VI. SIMULATION STUDY

Numerical simulation studies have been conducted to evaluate the performance of the proposed longitudinal wheel-slip controller before experiments on real vehicle are carried out. The mathematical models and parameters presented in Section II are used in the simulations. To imitate the real world measurement, normal distribution noise with amplitude 0.01 is added in the measurements of vehicle body acceleration and wheel speed.

In order to cover different scenarios, varying situations in three different aspects, that are, target torque, steering command, and road condition have been applied on each wheel simultaneously in the simulation.

Target torque: Each wheel is subjected to different kinds of target torque as shown in Fig. 5.

Steering command: Varying steering command is also imposed to the vehicle and it is set as

$$\begin{cases} \phi_1 = \frac{\pi}{8}\sin 0.2t \\ \phi_2 = 0 \\ \phi_3 = 0 \end{cases} \tag{19}$$

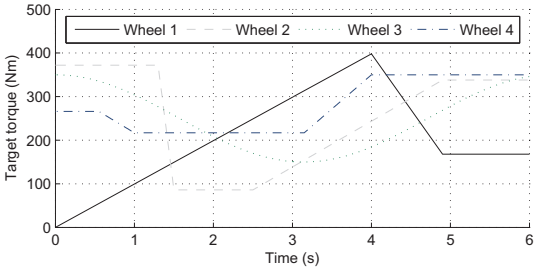

Fig. 5. Target torque of each wheel in the simulation.

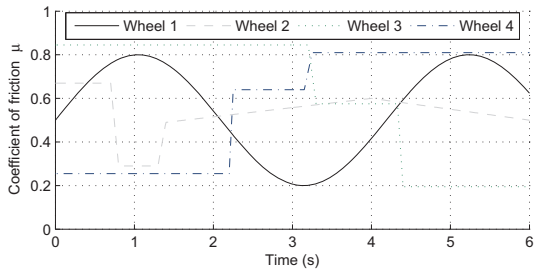

Fig. 6. Different road conditions on each wheel.

It makes the location of the target ICR changes along y-axis periodically. It means that the vehicle is commanded to turn left and right periodically.

Road condition: Each wheel is also subjected to different and varying road conditions. To ease for generating different road conditions in the simulation, the parameters in (4) are changed according to the coefficient of friction μ by,

$$f(\sigma_i) = \hat{D}\sin(C\arctan\{\hat{B}\sigma_i - E[\hat{B}\alpha - \arctan(\hat{B}\sigma_i)]\}) \tag{20}$$

where $\hat{D} = \mu D$ and $\hat{B} = \sqrt{\mu}B$. Fig. 6 illustrates the different road conditions imposed on each wheel in terms of the coefficient of friction μ.

Fig. 7 shows the torque commands controlled by the proposed longitudinal wheel-slip controller on each wheel under those varying conditions. It shows that the torque command follows the target torque when the torque is not over the limit. The torque commands are chattering in certain periods as the target torques of that periods were higher than the torque limit that a serious slip may occur. The controller tries to suppress the wheel slip by the chatting torque pattern. The slip ratio of each wheel is showed in Fig. 9. It can be observed that the slip ratio is suppressed under 0.2 which within the adhersion area of the tires. The linear speed of the wheels and the vehicle body are shown in Fig. 11. It shows that the linear speeds of wheels are always close to the speed of the vehicle body.

To demonstrate the difference between the performance of the proposed and the conventional longitudinal wheel-slip detector when applying on 4WISD vehicles, another simulation has been conducted under the same conditions except the proposed longitudinal wheel-slip detector is replaced by the conventional longitudinal wheel-slip detector (13). Fig. 8 and Fig. 10 shows the resultant output torque and wheel

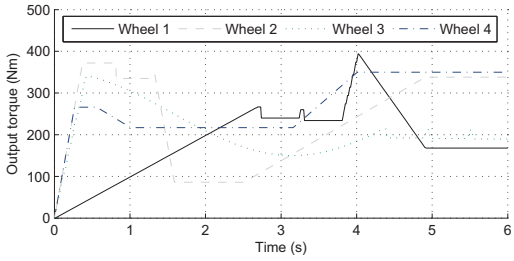

Fig. 7. Torque commands controlled by the proposed longitudinal wheel-slip controller.

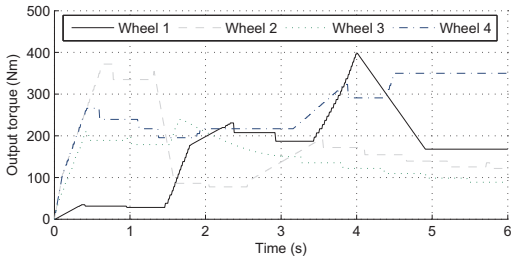

Fig. 8. Torque commands by using the conventional longitudinal wheel-slip detector.

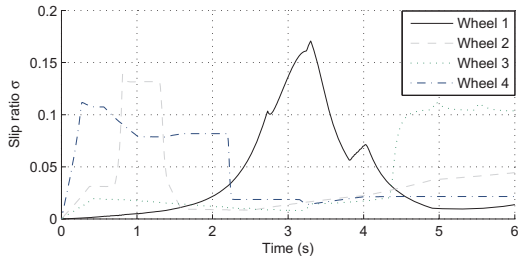

Fig. 9. Actual slip ratio on each wheel by using the proposed longitudinal wheel-slip controller.

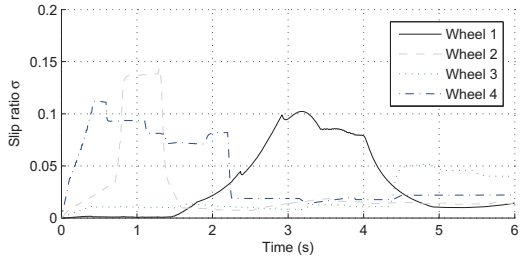

Fig. 10. Actual slip ratio on each wheel by using the conventional longitudinal wheel-slip controller.

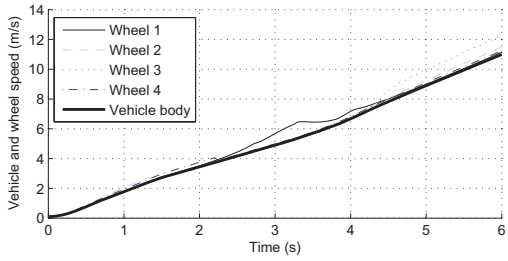

Fig. 11. Linear speed of wheels and the vehicle body by using the proposed longitudinal wheel-slip controller.

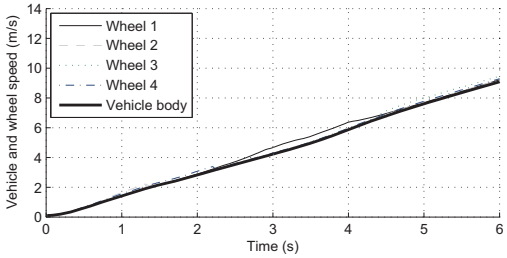

Fig. 12. Linear speed of wheels and the vehicle body by using the conventional longitudinal wheel-slip detector.

slip on each wheel respectively. It can be observed that although serious wheel slip did not occurred, some of the output torques were decreased when compare with Fig. 7 as the longitudinal wheel slip detector detect the longitudinal wheel slip wrongly. The wrong detection is mainly due to the neglect of the coupling effect of the traction force from other wheels. Fig. 12 illustrates the resultant speed of the vehicle. It shows that the vehicle speed at 6th second is about 9m/s, where the vehicle speed is around 11m/s when using the proposed method (Fig. 11). The comparison shows that the proposed method permits the vehicle run faster without serious slip.

In summary, the simulation results reveal the significance of the proposed longitudinal wheel-slip detector and shows the effectiveness of the proposed longitudinal wheel-slip controller in suppressing slip in all wheels in spite of the variation of target torque, steering command, and road condition.

VII. Conclusion

The contributions of this paper are summarized as follows. We have proposed a generalized longitudinal wheel-slip detector which considers the independent traction force of all wheels and omni-directional steering command. It can be applied on vehicles with an arbitrary quantity of driving wheels and different steering configurations. An inertial-based re-adhesion detector is also proposed to estimate the slip ratio by using an accelerometer. With the use of the proposed longitudinal wheel-slip detector and the inertial-based re-adhesion detector, a longitudinal wheel-slip controller is proposed to suppress all wheels slip in 4WISD vehicles. Simulation results reveal the effectiveness of the proposed controller in different road conditions, target torques and steering commands. In addition, the proposed method permits a vehicle run faster without serious slips when compare with the conventional method.

In the future, both the normal, longitudinal and lateral tire forces will be considered at the same time in the proposed controller to deal with the actual situation. The advanced controller will then be applied on a 4WISD vehicle to evaluate the actual performance.

References

[1] Kai Zheng, Tielong Shent, and Yu Yaot, "A Robust Nonlinear Control Approach for the Traction Problem in Electrical Vehicles", *IEEE Vehicle Power and Propulsion Conference*, pp. 1-5, September 6-8, 2006.

[2] M. Amodeo, A. Ferrara, R. Terzaghi, and C. Vecchio, "Wheel Slip Control via Second-Order Sliding-Mode Generation", *IEEE Transactions on Intelligent Transportation Systems*, Vol. 11, No. 1, pp.122-131, March 2010.

[3] D. Bevly, J. Gerdes, and C. Wilson, "The use of GPS based velocity measurements for measurement of sideslip and wheel slip" , Veh. Syst. Dyn., vol. 38, no. 2, pp. 127-147, Feb. 2003.

[4] M. Joos, J. Ziegler, C. Stiller. "Low-Cost Sensors for Image Based Measurement of 2D Velocity and Yaw Rate", *IEEE Intelligent Vehicles Symposium (IV)*, San Diego, CA, USA., pp. 658 - 662, June 21-24, 2010.

[5] Yoichi Hori, Yasushi Toyoda, and Yoshimasa Tsuruoka, "Traction Control of Electric Vehicle Basic Experimental Results Using the Test EV UOT Electric March", *IEEE Transactions on Industry Applications*, vol. 34, no. 5, September/October 1998.

[6] Kiyoshi Ohishi, Ken Nakano, Ichiro Miyashita, Shinobu Yasukawa, "Anti-Slip Control of Electric Motor Coach Based on Disturbance observer", *5th International Workshop on Advanced Motion Control*, Coimbra, pp. 580-585, 29 Jun-1 Jul 1998.

[7] Shin-ichiro Sakai, Hideo Sado, and Yoichi Hori, "Motion Control in an Electric Vehicle with Four Independently Driven In-Wheel Motors", it IEEE/ASME Transactions on Mechatronics, Vol. 4, No. 1, pp. 9-16, March 1999.

[8] Dejun Yin, and Yoichi Hori, "A Novel Traction Control of EV Based on Maximum Effective Torque Estimation", *IEEE Vehicle Power and Propulsion Conference*, Harbin, China, pp.1-6, September 3-5, 2008.

[9] K. Ohishi, T. Hata, T. Sano, and S. Yasukawa, "Realization of Anti-slip/skid Re-adhesion Control for Electric Commuter Train Based on Disturbance Observer", *IEEJ Transactions on Electrical and Electronic Engineering*, Vol. 4, No. 2, pp. 199-209, 2009.

[10] M. Lauria, et al, "Design and control of a four steered wheeled mobile robot", *IEEE 32nd Annual Conference on Industrial Electronics*, pp.4020-4025, Nov. 6-10, 2006.

[11] J. Yamakawa, and K. Watanabe, "A method of optimal wheel torque determination for independent wheel drive Vehicles", *Journal of Terramechanics*, Vol. 43, Issue 3, pp. 269-285, July 2006.

[12] S. Sakai, H. Sado, Y. Hori, "Dynamic driving/braking force distribution in electric vehicles with independently driven four wheels", *Electrical Engineering in Japan*, Vol. 138, No. 1, 2002.

[13] F. Tahami, R. Kazemi, and S. Farhanghi, "A novel driver assist stability system for all-wheel-drive electric vehicles", *IEEE Transactions on vehicular Technology*, Vol. 52, No.3, pp. 683-692, May 2003.

[14] R. P. Osborn, and T. Shim, "Independent control of all-wheel drive torque distribution", *Vehicle System Dynamics*, Vol. 44, No. 7, pp. 529-546(18), July 2006.

[15] T. Lam, Y. Xu, and G. Xu, "Traction Force Distribution on Omni-directional Four Wheel Independent Drive Electric Vehicle", *2009 IEEE International Conference on Robotics and Automation*, Kobe, Japan, pp.3724-3729, May 12-17, 2009.

[16] H. Qian, T. Lam, W. Li, C. Xia, and Y. Xu, "System and Design of an Omni-directional Vehicle", *Proceedings of the IEEE International Conference on Robotics and Biomimetics*, Bangkok, Thailand, pp. 389-394, Dec. 14-17, 2008.

[17] R. Siegwart, I. R. Nourbakhsh. " Introduction to autonomous mobile robots", *MIT Press*, April 2004.

[18] T. Lam, H. Qian, and Y. Xu, "Omnidirectional Steering Interface and Control for a Four-Wheel Independent Steering Vehicle", *IEEE/ASME Transactions on Mechatronics*, Vol. 152, No. 3, pp. 329-338, June 2010.

[19] E. Bakker, L. Nyborg, H. Pacejka, "Tire modelling for use in vehicle dynamics studies", *Society of Automotive Engineers*, 400 Commonwealth Dr., Warrendale, PA 15096, Jan. 1, 1987.

[20] H. Fujimoto, A. Tsumasaka, and T. Noguchi, "Direct yaw-moment control of electric vehicle based on cornering stiffness estimation", *31st Annual Conference of the IEEE Industrial Electronics Society*, North Carolina, USA, pp. 2626-2631, Nov. 6-10, 2005.